

Estimation of Elasticity and Viscosity in Heterogeneous Medium using FDTD Method and AHI Algorithm

Quang–Hai Luong
Le Quy Don Technical University
Hanoi, Vietnam
Email: luonghai@mta.edu.vn

Duc–Tan Tran, Linh–Trung Nguyen
VNU University of Engineering and Technology
Hanoi, Vietnam
Email: tantd,linhtrung@vnu.edu.vn

Tue Huu Huynh
International University
Ho Chi Minh City, Vietnam
Email: hhtue@hcmiu.edu.vn

Abstract—Mechanical properties of tissues in terms of elasticity and viscosity provide us useful information which may be used in detecting tumors. These parameters can be estimated from the measurement of particle velocities of shear wave propagation which is generated by a vibrating needle at a certain frequency. For the heterogeneous medium, the finite difference time domain (FDTD) is an effective method to present the shear wave propagation. The elasticity and viscosity are then estimated using the algebraic Helmholtz inversion (AHI) algorithm. However, there is a lack of deep investigation of estimation by combining FDTD method and AHI algorithm. Thus, this paper presents a complete system which includes the principle of excitation and measurement, the FDTD to model the shear wave propagation, the AHI algorithm to estimate the elasticity and viscosity, and the investigation on frequency-dependent the elasticity and viscosity. Also, we suggest that the excitation frequency of 200 Hz will offer the best estimation of the elasticity and viscosity.

I. INTRODUCTION

Mechanical properties of tissues in terms of elasticity and viscosity provide us useful information which may be used in medical diagnosis, especially in detecting tumors [1]. Among various elasticity imaging modalities, ultrasonic shear wave elasticity imaging (SWEI), introduced in 1998 by Sarvazyan *et al.* [2], is used for estimating the complex shear modulus (CSM) of biphasic hydro polymers including soft biological tissues. As a consequence, SWEI can be coupled with traditional (e.g., structural) ultrasound imaging to provide additional information in the diagnosis. In a recent survey on different state-of-art techniques of ultrasound elastography [3], Gennisson *et al.* have confirmed that SWEI has significant advantages over the other techniques in terms of reproducibility, quantification, elasticity contrast, and automatic shear wave generation. These advantages lead to new applications of SWEI, not only for diagnosis but also for treatment [4], [5], [6] and [7].

With respect to CSM estimation, various methods have been developed as briefly surveyed next. In 2004, by using the fact that propagation speed of shear waves is related to the frequency of vibration, the elasticity and viscosity of the medium Chen *et al.* proposed a method to estimate the shear elasticity and viscosity of a homogeneous medium by measuring the shear wave speed dispersion and, in turns, the

CSM [8]. In 2007, Zheng *et al.* applied a linear Kalman filter for the reconstruction of the harmonic motion of particle velocities at distinct spatial locations [9]. Their approach is to model displacement at the spatial points of interest as a sinusoidal function of time. From estimated quantities, absolute phase at a distinct spatial location can be found. By repeating the same procedure for another location a phase difference is found. Shear wave speed and shear wave dispersion curves are estimated over a frequency bandwidth and material properties are obtained. In 2008, Liu and Ebbini proposed a second-order dynamical model to reconstruct the CSM for thin tissue constructs [10]. Their approach was to displace a tissue construct at the distinct spatial location by using acoustic radiation force. They track tissue displacement and use an EKF approach to reconstruct material properties at the given location. The EKF approach is necessary since the dynamical model used is a non-linear function of the underlying material parameters. Because they use acoustic radiation force to generate shear waves, so a drawback of this method is difficult to determine the force magnitude which needs to be known for the calculations. In 2010, Orescanin *et al.* have conducted an experiment whereby they modeled the nonlinear relationship between wave dynamics and material parameters. They represented the CSM parameters of the present by a nonlinear function of the CSM parameters in the past. So, they applied the Maximum Likelihood Ensemble Filter (MLEF), which is a stochastic filter capable of handling nonlinear dynamical models and nonlinear observation operators, to estimate the CSM of a homogeneous medium based on the Kelvin–Voigt model [11]. For the problem of tumor detection, in 2013, this MLEF approach was extended to a one-dimensional (1D) heterogeneous medium by Tran *et al.* [12] and a two-dimensional (2D) heterogeneous medium by Hao *et al.* [13]. However, the limitation of works in [11], [12], and [13] is that authors use the wave equation for shear wave propagation. It works well with homogeneous medium but not in heterogeneous one. For the heterogeneous medium, the finite difference time domain (FDTD) is an effective method to present the shear wave propagation. The elasticity and viscosity are then estimated using the algebraic

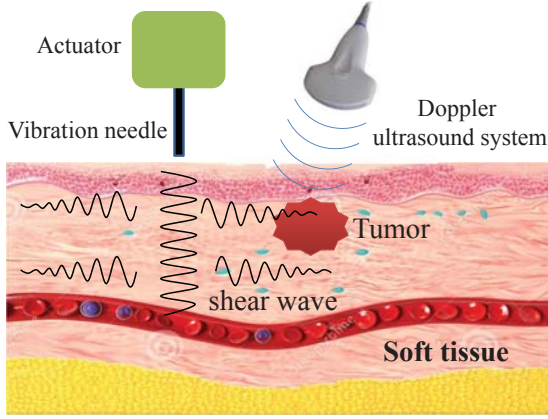


Fig. 1. Generation and measurement shear wave.

Helmholtz inversion (AHI) algorithm. However, there is a lack of deep investigation of estimation by combining FDTD method and AHI algorithm. Thus, this paper presents a complete system which includes the principle of excitation and measurement, the FDTD to model the shear wave propagation, the AHI algorithm to estimate the elasticity and viscosity, and the investigation on frequency-dependent the elasticity and viscosity. Also, we suggest that the excitation frequency of 200 Hz will offer the best estimation of the elasticity and viscosity.

II. METHOD

A. Shear wave propagation

Shear wave is generated and measured as illustrating to Figure 1. A mechanical actuator was adapted to hold a stainless-steel needle. The needle is 1.5 mm in diameter and 13 cm long. It is controlled to generate a vibration along the z-axis at a frequency in the range of 50 Hz to 450 Hz (in this research, the chosen frequency is 200 Hz). Consequently, the shear wave is propagated in the perpendicular plane (i.e. x- and y-axes). After that, a Doppler ultrasound system was used to measure the particle velocity [11].

In some studies ([11], [12] and [13]), the authors used wave equation (1) to represent the shear wave propagation in tissues. In which, the particle velocity $v(r, t)$ of shear wave at a point is a spatial-temporal function of the radial distance r and time t , and is given by

$$v(r, t) = \frac{1}{\sqrt{r - r_0}} A e^{-\alpha(r - r_0)} \cos[\omega t - k_s(r - r_0) - \phi], \quad (1)$$

where A is the amplitude of source excitation, r_0 is the needle position, and ϕ is the initial temporal phase, α and k_s are attenuation coefficient and wave number at surveyed point. However, this approach shows that the particle velocity at each point in space is independent with each other, it only depends on parameters of medium. This is not accurate, because, in fact, the particle velocity at a point in space depends on one

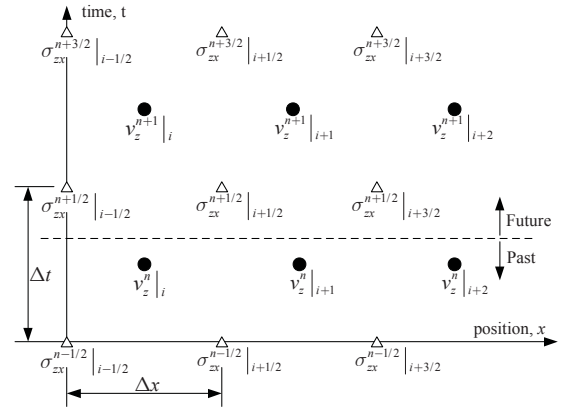


Fig. 2. The arrangement of stress tensor σ and velocity vector v_z nodes in space and time. The stress tensor nodes are shown as triangles and the velocity vector nodes as circles.

of its pre-point on the direction of propagation, especially in a heterogeneous medium.

In this paper, we applied the FDTD model for the shear wave propagation in tissues. Under the assumption of cylindrical shear wave propagation along the radial axis and ignoring absorption of medium, the particle velocity vector v_z on a direction of the wave propagation x in cartesian coordinate relates to the stress tensor σ_{zx} following Eqs. (2) and (3) [14].

$$\rho \partial_t v_z = \partial_x \sigma_{zx}, \quad (2)$$

$$\partial_t \sigma_{zx} = (\mu + \eta \partial_t) \partial_x v_z, \quad (3)$$

where ∂_t represents a partial derivative operator $\partial/\partial t$ applied to values to the right of the symbol, ∂_x represents a partial derivative operator $\partial/\partial x$ applied to values to the right of the symbol, ρ is mass density of medium (tissues), μ and η are the elasticity and viscosity of medium.

According to the Kelvin-Voigt model, the CSM $G(x, \omega)$ is defined as

$$G(x, \omega) = \mu(x) - i\omega\eta(x), \quad (4)$$

where ω is the angle frequency of the vibration. Thus the CSM estimation means estimating the elasticity μ and the viscosity η .

The next step is to replace the derivatives in (2) and (3) with finite differences. To do this, space and time need to be discretized. The following notation will be used to indicate the location where the fields are sampled in space and time

$$v_z(x, t) = v_z(i\Delta x, n\Delta t) = v_z^n |_{i}, \quad (5)$$

$$\sigma_{zx}(x, t) = \sigma_{zx}(i\Delta x, n\Delta t) = \sigma_{zx}^n |_{i}, \quad (6)$$

where Δx is the spatial offset between sample points and Δt is the temporal offset. The index i corresponds to the spatial step, while the index n corresponds to the temporal step.

Figure 2 shows sample points, also known as nodes, in spatial dimension and time dimension. Base on the FDTD

approach, we expressed (2) and (3) in discrete form as follows:

$$v_z^{n+1} |_i = v_z^n |_i + \frac{\Delta t}{\rho \Delta x} \left(\sigma_{zx}^{n+\frac{1}{2}} |_{i+\frac{1}{2}} - \sigma_{zx}^{n+\frac{1}{2}} |_{i-\frac{1}{2}} \right), \quad (7)$$

$$\sigma_{zx}^{n+\frac{1}{2}} |_{i+\frac{1}{2}} = \sigma_{zx}^{n-\frac{1}{2}} |_{i+\frac{1}{2}} + \frac{\mu \Delta t}{\Delta x} (v_z^{n+1} |_{i+1} - v_z^{n+1} |_i) + \frac{\eta}{\Delta x} (v_z^{n+1} |_{i+1} - v_z^{n+1} |_i) - \frac{\eta}{\Delta x} (v_z^n |_{i+1} - v_z^n |_i), \quad (8)$$

To show the difference between the propagation model (1) and FDTD model, we built an unique simulation scenario and applied these both methods to compute the particle velocity at each spatial locations. The simulation scenario consists of two cases: i) a 1D homogeneous medium which consist of 200 points with the same CSM; ii) a 1D heterogeneous medium which consist of 200 points, the CSM value is changed gradually from the 55th point to the 79th point. Figure 3 shows the particle velocity in spatial locations in both mediums when using wave equation (1), while Figure 4 shows one using the FDTD model. For a 1D heterogeneous medium, Figure 3 shows that at the 55th point, the CSM value is changed suddenly. The particle velocities in Fig. 3 are clearly different. Thus, it would be easy to estimate CSM. However, the particle velocity (dotted curve) shown in Fig. 3 does not reflect the real particle velocity in heterogeneous medium. The dotted curve in Figure 4 presents real the particle velocity in heterogeneous medium which is changed more smoothly. However, accurate estimation of the CSM would be a challenge.

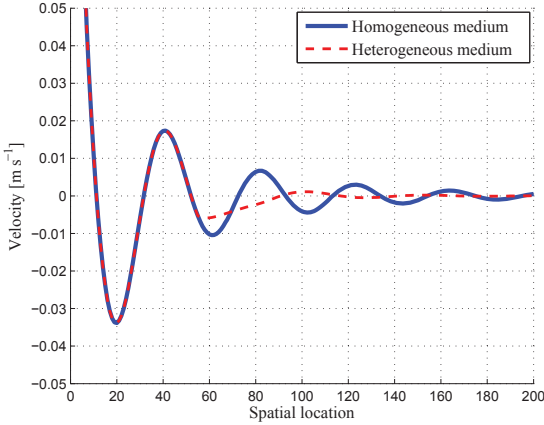


Fig. 3. The particle velocity in space, using wave equation (1).

B. Direct inversion to estimate the CSM

In this section, we applied the AHI algorithm [15] to estimate the CSM from the spatial patterns of simulated shear waves. In a small range, we assumed that the viscoelastic properties of the medium are isotropic and there is negligible compression applied to the medium by the source, then the particle velocity vector v_z can be described by the Navier

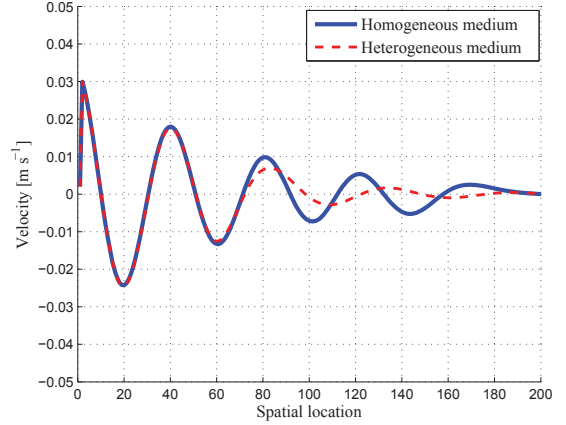


Fig. 4. The particle velocity in space, using FDTD model.

wave equation in a homogeneous solid, which is obtained by combining equations in (2) and (3),

$$\rho \frac{\partial^2 v_z}{\partial t^2} = G'(x, t) \nabla^2 v_z, \quad (9)$$

where $G'(x, t)$ is the CSM in time domain, $\nabla^2 v_z$ is Laplace operator of v_z and defined as $\nabla^2 v_z = \partial^2 v_z / \partial x^2$.

Applying the AHI algorithm to solve (9), then Eq. (9) becomes the Helmholtz equation

$$\left(\frac{G(x, \omega)}{\rho} \nabla^2 + \omega^2 \right) V_z(x, \omega) |_{\omega=\omega_0} = 0, \quad (10)$$

where $G(x, \omega)$ is the CSM in frequency domain and defined in (4), $V_z(x, \omega)$ is the temporal Fourier transform of the particle velocity $v_z(x, t)$, $V_z(x, \omega) = F_t \{v_z(x, t)\}$, ω_0 is only the value at the determined frequency of the vibration. From (10), we can see that the CSM can be estimated directly as

$$\mu(x) = \Re \left\{ \frac{-\rho \omega_0^2 V_z(x, \omega_0)}{\nabla^2 V_z(x, \omega_0)} \right\}, \quad (11)$$

$$\eta(x) = \Im \left\{ \frac{-\rho \omega_0 V_z(x, \omega_0)}{\nabla^2 V_z(x, \omega_0)} \right\}.$$

We propose a procedure to verify the quality of CSM estimation by changing the excitation frequency. The procedure is summarized as following:

- 1) Initiation, $i = 1$
- 2) Select the excitation frequency $\omega_0 = 150$,
- 3) Vibrate the needle to generate shear waves,
- 4) Measure the particle velocity using a Doppler ultrasound system,
- 5) Estimate CSM in 120 spatial locations using Equ.(10),
- 6) Assign $i = i + 1$, $\omega_0 = \omega_0 + 50$,
- 7) Return to step 3 if $i < 4$; stop if $i > 4$.

III. RESULTS AND DISCUSSIONS

To test the proposed method, we built a simulation scenario as follows: The 1D heterogeneous medium is 20 mm in size;

the elasticity and viscosity of medium are respectively 650 Pa and 0.1 Pa.s from 0 to 5.5 mm, 900 Pa and 0.35 Pa.s from 8 to 20 mm, and from 5.5 to 8 mm the elasticity grows from 650 to 900 Pa, the viscosity grows 0.1 to 3.5 Pa.s; the frequency of the vibration is 200 Hz; the amplitude of the vibration is 2 mm.

We applied FDTD model to simulate the shear wave propagation in tissues. In there, we divided the medium into 200 points ($\Delta x = 0.1$ mm), at each point we took 2000 samples with $\Delta t = 0.01$ ms. Figure 5 shows the particle velocity in term of time at the 2nd point. It presents a sinusoidal function of time. Figure 6 indicates the particle velocity in space. It shows the particle velocity attenuated strongly from 120th point, so we only implemented the CSM estimation from 1st point to 120th point.

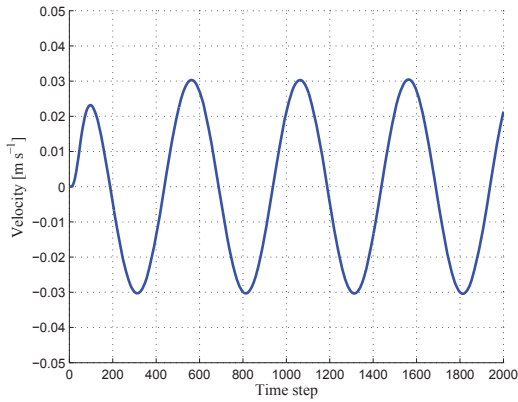


Fig. 5. The particle velocity in time at the 2nd point.

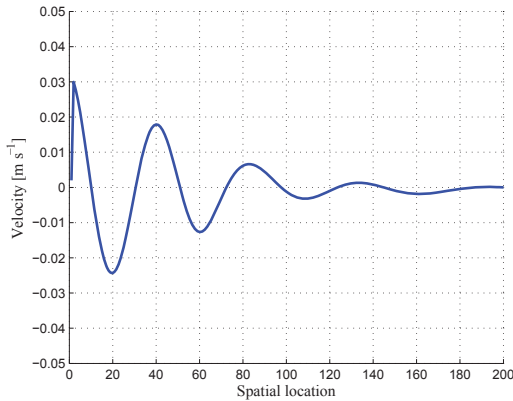


Fig. 6. The particle velocity in space.

We implemented estimating the CSM with some frequencies of the vibration 150 Hz, 200 Hz and 250 Hz, after, we showed all of the received results on a chart. Figures 7 and 8 indicate The estimated elasticity and viscosity, respectively, with different frequencies of the vibration. The results show that the quality of the CSM estimation is best at frequency

200 Hz. Results shows that the estimated elasticity follows closely the ideal elasticity, especially in range, from 1st point to 55th point. This is explained that the Navier wave equation (9) is applied very well in a homogeneous medium. For a heterogeneous medium, the CSM estimation obtain more error.

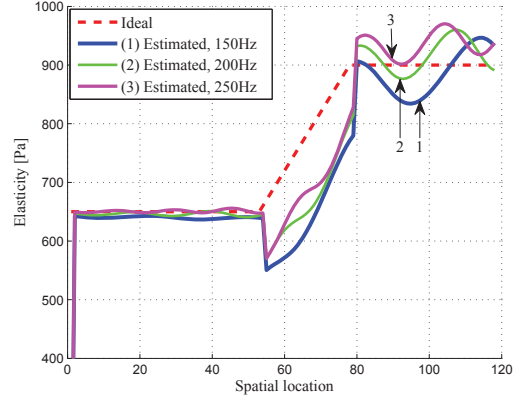


Fig. 7. The estimated elasticity, with different frequencies of the vibration.

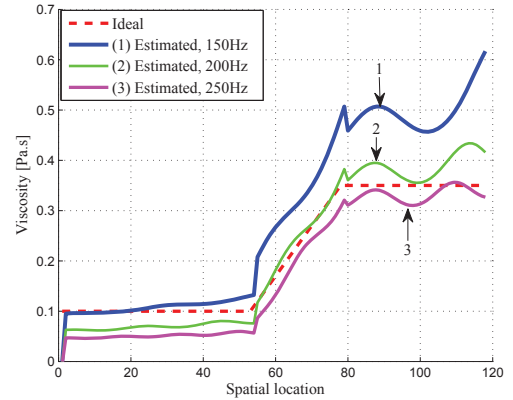


Fig. 8. The estimated viscosity, with different frequencies of the vibration.

We used the maximum error to evaluate the quality of the CSM estimation on ranges of medium. The results are illustrated in Table I.

TABLE I
MAXIMUM ERROR OF THE CSM ESTIMATION

Points	Maximum error for elasticity [Pa]	Maximum error for viscosity [Pa.s]
1–55	± 9.2	± 0.038
56–79	± 136.3	± 0.02
80–120	± 86	± 0.08

IV. CONCLUSION

This paper presents a complete system which includes the principle of excitation and measurement, the FDTD to model

the shear wave propagation, the AHI algorithm to estimate the elasticity and viscosity, and the investigation on frequency-dependent the elasticity and viscosity. Our method only requires a single vibration frequency to accurately estimate the elasticity and viscosity. In this experiment, we tested with some vibration frequencies (150 Hz, 200 Hz and 250 Hz) and suggested that the excitation frequency of 200 Hz will offer the best estimation of the elasticity and viscosity. CSM is estimated at each spatial location, then expanding to a series of spatial locations on a ray (i.e 1-D reconstruction). In future work, we will apply the Bayesian-approach-based Maximum Likelihood Ensemble Filter (MLEF) to CSM estimation where FDTD is exploited to build the system model. It would perform well in both homogeneous tissue-like materials and materials with inclusions. This will facilitate clinical diagnoses such as cancer detection.

REFERENCES

- [1] J. Bercoff, A. Criton, C. Bacrie, J. Souquet, M. Tanter, J. Gennisson, T. Defieux, M. Fink, V. Juhán, A. Colavolpe *et al.*, "ShearWave Elastography A new real time imaging mode for assessing quantitatively soft tissue viscoelasticity," in *Ultrasonics Symposium, 2008. IUS 2008. IEEE*. IEEE, 2008, pp. 321–324.
- [2] A. P. Sarvazyan, O. V. Rudenko, S. D. Swanson, J. B. Fowlkes, and S. Y. Emelianov, "Shear wave elasticity imaging: a new ultrasonic technology of medical diagnostics," *Ultrasound in medicine & biology*, vol. 24, no. 9, pp. 1419–1435, 1998.
- [3] J.-L. Gennisson, T. Defieux, M. Fink, and M. Tanter, "Ultrasound elastography: principles and techniques," *Diagnostic and interventional imaging*, vol. 94, no. 5, pp. 487–495, 2013.
- [4] G. Ferraioli, P. Parekh, A. B. Levitov, and C. Filice, "Shear wave elastography for evaluation of liver fibrosis," *Journal of Ultrasound in Medicine*, vol. 33, no. 2, pp. 197–203, 2014.
- [5] Y. Kobayashi, M. Tsukune, T. Miyashita, and M. G. Fujie, "Simple empirical model for identifying rheological properties of soft biological tissues," *arXiv preprint arXiv:1509.02021*, 2015.
- [6] S. Woo, S. Y. Kim, M. S. Lee, J. Y. Cho, and S. H. Kim, "Shear wave elastography assessment in the prostate: an intraobserver reproducibility study," *Clinical imaging*, vol. 39, no. 3, pp. 484–487, 2015.
- [7] W. Zhang and S. Holm, "Estimation of shear modulus in media with power law characteristics," *Ultrasonics*, vol. 64, pp. 170–176, 2016.
- [8] S. Chen, M. Fatemi, and J. F. Greenleaf, "Quantifying elasticity and viscosity from measurement of shear wave speed dispersion," *The Journal of the Acoustical Society of America*, vol. 115, no. 6, pp. 2781–2785, 2004.
- [9] Y. Zheng, S. Chen, W. Tan, R. Kinnick, and J. Greenleaf, "Detection of tissue harmonic motion induced by ultrasonic radiation force using pulse-echo ultrasound and kalman filter," *Ultrasonics, Ferroelectrics, and Frequency Control, IEEE Transactions on*, vol. 54, no. 2, pp. 290–300, 2007.
- [10] D. Liu and E. S. Ebbini, "Viscoelastic property measurement in thin tissue constructs using ultrasound," *Ultrasonics, Ferroelectrics, and Frequency Control, IEEE Transactions on*, vol. 55, no. 2, pp. 368–383, 2008.
- [11] M. Orescanin and M. F. Insana, "Model-based complex shear modulus reconstruction: A Bayesian approach," in *IEEE Ultrasonics Symposium (IUS)*. IEEE, 2010, pp. 61–64.
- [12] T. Tran-Duc, Y. Wang, N. Linh-Trung, M. N. Do, and M. F. Insana, "Complex Shear Modulus Estimation Using Maximum Likelihood Ensemble Filters," in *4th International Conference on Biomedical Engineering in Vietnam*. Springer Berlin Heidelberg, 2013, pp. 313–316.
- [13] N. T. Hao, T. Thuy-Nga, V. Dinh-Long, T. Duc-Tan, and N. Linh-Trung, "2D Shear Wave Imaging Using Maximum Likelihood Ensemble Filter," in *International Conference on Green and Human Information Technology (ICGHIT 2013)*. IEEE, 2013, pp. 88–94.
- [14] M. Orescanin, Y. Wang, and M. F. Insana, "3-d ftd simulation of shear waves for evaluation of complex modulus imaging," *IEEE transactions on ultrasonics, ferroelectrics, and frequency control*, vol. 58, no. 2, pp. 389–398, 2011.
- [15] S. Papazoglou, U. Hamhaber, J. Braun, and I. Sack, "Algebraic helmholtz inversion in planar magnetic resonance elastography," *Physics in medicine and biology*, vol. 53, no. 12, p. 3147, 2008.